Photochemical & Photobiological Sciences (2022) 21:835–847
https://doi.org/10.1007/s43630-021-00166-z

ORIGINAL PAPERS

UV-induced –OCH_3 rotamerization in a matrix-isolated methoxy-substituted *ortho*-hydroxyaryl Schiff base

İsa Sıdır[1,2] · Yadigar Gülseven Sıdır[1,2] · Sándor Góbi[2,3] · Halil Berber[4] · Gulce Ogruc Ildiz[5] · Rui Fausto[2]

Received: 29 October 2021 / Accepted: 27 December 2021 / Published online: 25 January 2022

Abstract

A new methoxy-substituted *ortho*-hydroxyaryl Schiff base, 4-(3-methoxy-2-hydroxybenzylidene-amino) phenol was synthesized from 4-aminophenol and 2-hydroxy-3-methoxybenzaldehyde in methanol solution and characterized by ^{1}H-NMR, ^{13}C-NMR and infrared spectroscopies and elemental analysis. The compound was isolated in a cryogenic (10 K) argon matrix, and the analysis of the infrared spectrum of the matrix-isolated compound revealed that it corresponds to the *E*-enol-imine isomeric form, with 3 different conformers being present in the matrix. These conformers share as common structural features the conformation of the free hydroxyl group (*trans* relatively to the *para*-substituent of the ring) and the presence of an OH···N intramolecular H-bond involving the methoxy-substituted phenol ring and the azomethine bridge, while they differ in the orientation of the methoxy-substituent group. The structures and relative energies of the conformers of the molecule, and relevant barriers for their interconversion were obtained through quantum chemical calculations, which were also used to calculate the infrared spectra of the different forms. Calculations were also carried out for the higher-energy *Z*-enol-imine and keto-amine forms of the compound. Upon UV (230 nm) irradiation, –OCH_3 rotamerization was observed, leading to conversion of the lowest energy conformer, where the methoxy group is aligned with the plane of the ring, into the other two conformers initially present in the matrix, in which the OCH_3 group is out-of-the-plane of the ring. As for other phenolic compounds previously studied, spontaneous quantum mechanical tunneling conversion of the *cis*-OH conformers present in the gas-phase into the three observed conformers was found to take place during matrix deposition.

Graphical abstract

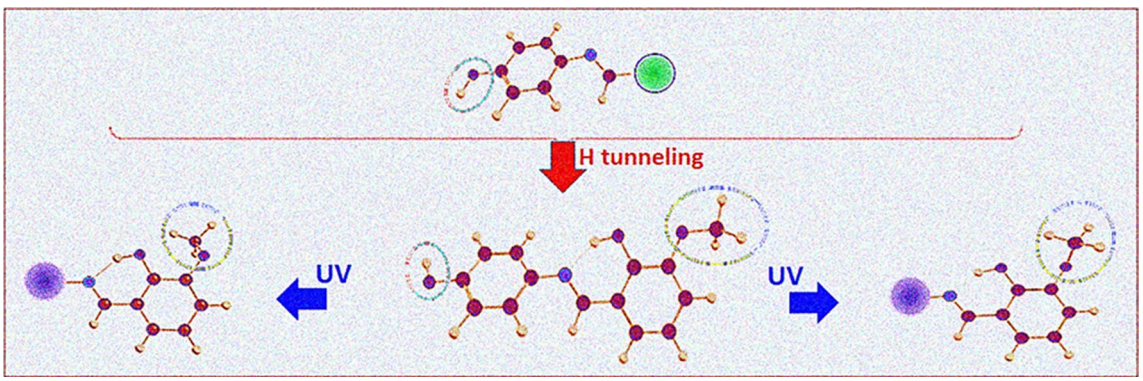

Keywords UV-induced –OCH_3 rotamerization · 4-(3-Methoxy-2-hydroxy-benzylideneamino) phenol · Matrix isolation · DFT(B3LYP)/6-311++G(d,p) calculations · Tunneling decay

Dedicated to Angelo Albini for his 75th birthday.

Extended author information available on the last page of the article

1 Introduction

In the last few years, we have reported a series of studies on Schiff base derivatives, including several compounds bearing the phenol moiety [1–5]. In the continuation of this series, we are now reporting on our investigation on 4-(3-methoxy-2-hydroxybenzylideneamino) phenol (abbreviated MHBAP). MHBAP is a member of the family of the *ortho*-hydroxyaryl Schiff bases, which are characterized structurally by having an *ortho* hydroxyl-substituted aromatic ring connected to the carbon atom of the Schiff base azomethine group (–N=CH–). These compounds are of great interest due to their wide range of practical applications, for instance as molecular switches [6, 7], sensors [8, 9] and for optical data storage devices [10–14]. They are versatile templates for molecular assembling, being also highly valued for fabrication of micro- and nanostructures [15–18].

Ortho-hydroxyaryl Schiff bases may exist in two tautomeric forms, enol-imine and keto-amine forms (Scheme 1), which are often easily interconvertible either thermally or photochemically [1–3, 19, 20]. Both enol-imine and keto-amine tautomers have two geometric isomers (*E* and *Z* forms), defined around the exocyclic C=N (in the enol-imine tautomer) or C=C (in the keto-amine tautomer) bond (see Scheme 1), which may also possess several conformational isomers depending on the substituents present in the molecule. A structural feature determining the relative energies of the different possible isomers of *ortho*-hydroxyaryl Schiff bases is the OH···N intramolecular hydrogen bond established between the *ortho*-OH group and the azomethine N atom in the *E*-enol-imine form, which has no equivalent in the other forms and usually makes this the dominant species [4, 5]. It has been shown that this intramolecular hydrogen bond makes the –N=CH–C=C–O–H fragment to assume a nearly planar arrangement, which is a particularly relevant structural property of *ortho*-hydroxyaryl Schiff bases, reducing the conformational freedom in the molecule, while allowing for significant electronic delocalization between the *ortho*-hydroxyaryl fragment and the azomethine group [4, 5, 21–23].

In the case MHBAP, the *ortho*-hydroxyaryl moiety bears a methoxy substituent vicinal to the hydroxyl group (in position 3 of the ring; see Scheme 2), which may assume different minimum energy orientations. In addition, the group connected to the N atom is a phenol group (bonded to the nitrogen at the *p*-position), and its OH moiety can also assume two possible orientations, herein designated as *cis* and *trans*, which correspond to the orientation of the OH group to the same side or to the opposite side of the N=C azomethine bond, respectively. These two conformational degrees of freedom in the MHBAP molecule can be expected to lead to several conformers of relatively similar energies.

The present study aimed to look in detail to the conformational space of MHBAP, with particular emphasis to the characterization of the lowest energy OH···N intramolecularly H-bonded forms of the compound. For this, matrix isolation infrared spectroscopy has been used together with density functional theory (DFT) calculations. Matrix isolation was used to trap the different conformers of the compound which have significant populations in the gas phase, which were shown to correspond exclusively to the OH···N intramolecularly hydrogen bonded conformers of the *E*-enol-imine form of MHBAP, while infrared spectroscopy was applied to their detection and characterization. The experimental studies were supported by extensive DFT calculations undertaken using the B3LYP functional and the split-valence triple-ς 6-311++G(d,p) basis set [24–29]. Besides, in situ narrowband UV irradiation of the matrix-isolated molecules was undertaken to induce conversions between the initially trapped conformers. We focused our attention on the rotamerization of the methoxy substituent and also on that of the OH free phenolic moiety of the molecule.

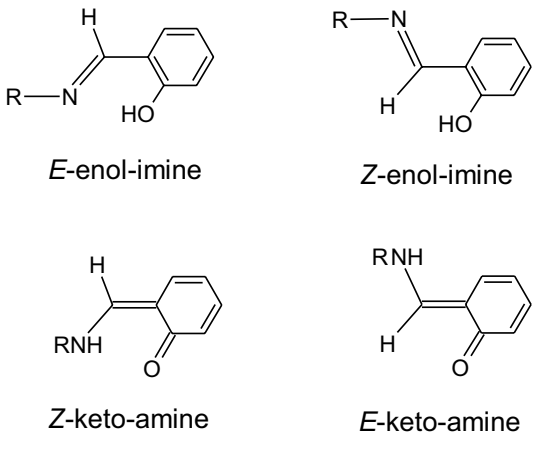

Scheme 1 Relevant tautomeric forms of *o*-hydroxyaryl Schiff bases. For MHBAP, R = *p*-phenol (see Scheme 2)

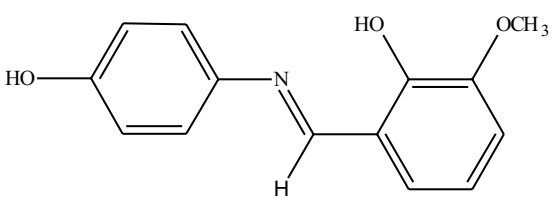

Scheme 2 Structure of MHBAP, in its *E*-enol-imine form

Scheme 3 Synthesis of MHBAP

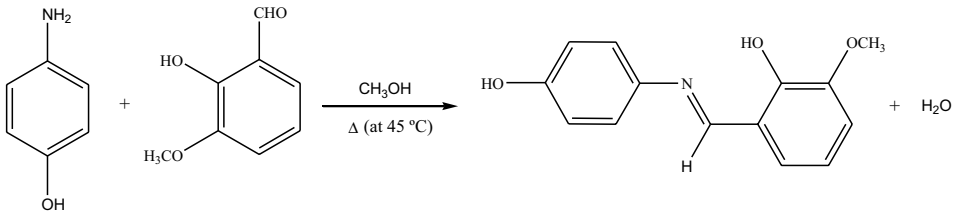

2 Experimental and computational methods

2.1 Synthesis

4-(3-Methoxy-2-hydroxybenzylideneamino) phenol was synthesized by mixing equivalent amounts of 4-aminophenol and 2-hydroxy-3-methoxybenzaldehyde in methanol solution, at ca. 45 °C (Scheme 3), following the general procedure previously reported [1–4].

4-Aminophenol (1.091 g, 0.01 mol) and 2-hydroxy-3-methoxybenzaldehyde (1.522 g, 0.01 mol) were first dissolved in 25 ml of methanol by heating, and the solutions were then added. After 1 h at ca. 45 °C, under slow stirring, the reaction completed and the precipitated product was filtered, purified by recrystallization from methanol, and dried in a vacuum desiccator at room temperature. The IR spectrum of the yellowish-orange purified crystalline material (in a KBr pellet at room temperature), and the ^{1}H- and ^{13}C-NMR spectra in deuterated dimethyl sulfoxide (DMSO-d_6) solution were found to be compatible with the desired product, and are provided as Supporting Material (Figures S1-S3). The IR spectrum was obtained in a Perkin Elmer FTIR 100 spectrometer, and the ^{1}H- and ^{13}C-NMR spectra in a Bruker Biospin Ultrashield™ 300 MHz NMR spectrometer, at room temperature. The melting point (m. p.) of the compound was measured using a Gallenkamp Sanyo Heater. Elemental analysis was performed using a CNHS-932 LECO apparatus. IR (KBr pellet, ν cm^{-1}): ~ 3627–3138 (O–H), ~ 3030–2935 (C–H, aromatic), ~ 2836–2607 (C-H, aliphatic), 1620 (C=N), 1457–1511 (C=C, aromatic), 1246 (C–O–C); ^{1}H-NMR (300 MHz, DMSO-d_6) δ 13.61 (s, 1H), 9.70 (s, 1H), 8.89 (s, 1H), 7.32 (d, J = 8.7 Hz, 2H), 7.18 (dd, J = 7.8, 1.3 Hz, 1H), 7.08 (dd, J = 8.0, 1.3 Hz, 1H), 6.90 (d, J = 7.9 Hz, 1H), 6.84 (d, J = 8.7 Hz, 2H), 3.81 (s, 3H); ^{13}C-NMR (75 MHz, DMSO-d_6) δ 160.82 (s), 157.44 (s), 150.83 (s), 148.30 (s), 139.44 (s), 124.11 (s), 123.10 (s), 119.77 (s), 118.88 (s), 116.43 (s), 115.46 (s), 56.29 (s); elemental analysis (calculated for $C_{14}H_{13}NO_3$)/observed: C, (69.12)/69.45; H, (5.39)/6.08; N, (5.76)/5.49. m.p. 148–151 °C.

2.2 Matrix isolation experiments

The matrices were prepared by sublimation of a solid sample of MHBAP, placed in a homemade Knudsen cell connected to the vacuum chamber of the cryostat, by deposition of the resulting vapors together with argon (Air Liquide, N60), in a matrix:solute approximate 1000:1 ratio, onto a cold (10.0 ± 0.1 K) CsI substrate. Cooling was undertaken using an APD DE-202A closed-cycle helium refrigeration system. The matrix isolation infrared spectra were recorded in the 4000–400 cm^{-1} range, with 0.5 cm^{-1} resolution, using a Nicolet 6700 FTIR spectrometer, equipped with a mercury cadmium telluride (MCT) detector and a KBr beam splitter. The instrument was purged by a stream of dry/CO_2-filtered air in order to avoid interference from atmospheric H_2O and CO_2 vapors.

UV irradiation (~ 15 mW at the sample) of the matrix-isolated compound was performed at λ = 230, 275 and 335 nm, close the absorption maxima of MHBAP in solution (see Figure S4; the fluorescence spectra of the compound in the different solvents is also provided, in Figure S5, showing maxima within the range 560–580 nm, depending on the used solvent), through the outer KBr windows of the cryostat, using a Spectra Physics MOPO-SL optical parametric oscillator (OPO; FWHM = 0.2 cm^{-1}) pumped by a pulsed (pulse duration 10 ns, repetition rate 10 Hz) Quanta Ray Pro-Series Nd-YAG laser (Figure S6).

2.3 Quantum chemical calculations

All calculations were carried out at the DFT(B3LYP) level of theory with 6-311++G(d,p) basis set [24–29] using GAUSSIAN 09 (revision C.01) [30]. The potential energy surfaces of four isomeric species (*E*-enol-imine, *Z*-enol-imine, *E*-keto-amine and *Z*-keto-amine; see Scheme 1) of MHBAP were systematically investigated, and the geometries of the identified minima were fully optimized using the standard convergence criteria of the program [30]. Relaxed potential energy profiles for the relevant internal rotations in the studied molecule were calculated at the same theory level.

The infrared spectra of the different conformers were also obtained (at the same theory level), within the harmonic approximation. To take into consideration the neglected an harmonic effects and limitations of the method and basis set, the harmonic vibrational wavenumbers were scaled by the factors 0.983 and 0.950, below and above 1800 cm^{-1}, respectively. Assignment of the vibrational spectra was carried out with the help of the animation module of ChemCraft (version 1.8) [31]. In the simulated spectra presented

in the figures, the IR bands were broadened by Lorentzian profiles (fwhm = 6 cm^{-1}) centered at the calculated (scaled) wavenumbers.

3 Results and discussion

3.1 Screening of MHBAP conformational space by DFT computations

Strictly speaking, monomers of the two enol-imine forms of MHBAP contain six distinct internal degrees of freedom that may give rise to different conformers, while the arrangement around the N=C azomethine double bond defines the nature of the enol form, *E* (C–C=N–C ~ 180°) or *Z* (C–C=N–C ~ 0°). From the six a priori conformationally relevant coordinates, two of them correspond to the internal rotations of the hydroxyl groups (defined by the dihedral angles α and β in Fig. 1), the third one to the internal rotation of the methoxy group (γ), and the fourth is defined by the dihedral angle ε (N = C–C=C). On the other hand, the rotation defined by the dihedral angle δ (C=C–N=C) leads to the same structures as those defined by the dihedral α, and is, in some sense, irrelevant in practical terms. Nevertheless, the barriers for the two different rotations (around the C–O and around the C–N bonds) that lead to the same structures are different, and were both evaluated in the present study. In turn, the internal rotation of the methyl group is a three-fold rotation and leads to three equivalent structures for each different orientations of the other moieties and it is, by this reason, not relevant in terms of definition of different conformers. In practical terms, the number of conformationally relevant coordinates reduces to only four.

In the performed conformational search for each one of the enol-imine forms of MHBAP, consideration of all the conformationally relevant degrees of freedom resulted in 16 distinct conformers, which are shown in Fig. 1 for the case of the more stable *E* form (the conformers of the *Z*-enol-imine form are shown in the Supporting Material Figure S7). The keto-amine forms (both *Z* and *E* forms) were predicted to have 12 different conformers each, which are also shown in the Supporting Material (Figure S8).

The energies (zero-point-corrected electronic energies) of the most stable conformer of the *Z*-enol-imine, *Z*-keto-amine and *E*-keto-amine forms were calculated to be 46.2, 16.0 and 54.8 kJ mol^{-1} higher than that of the most stable conformer of the *E*-enol-imine form, respectively. The energies of the different conformers of these three high-energy forms of MHBAP are given in Table S1 (Supporting Material). Table 1 shows the calculated relative electronic energies

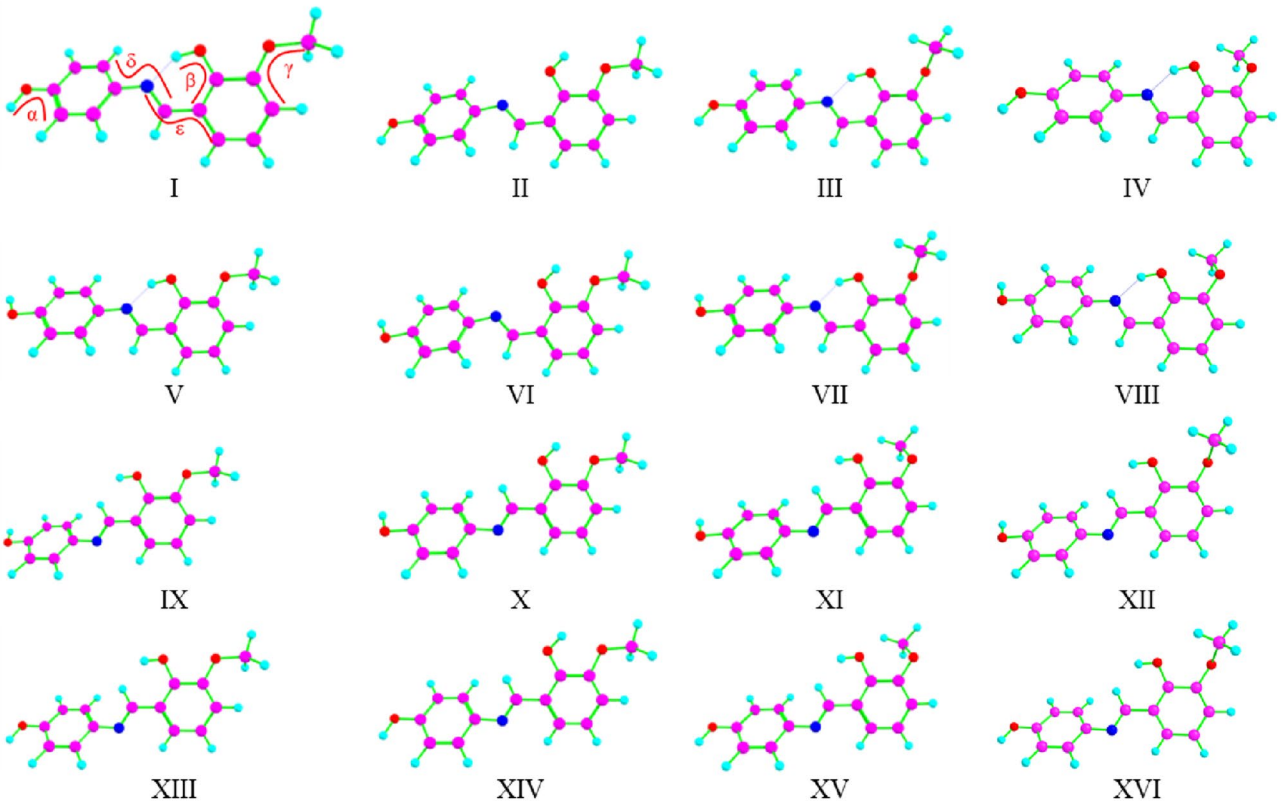

Fig. 1 Conformers of MHBAP, in its *E*-enol-imine form

Table 1 B3LYP/6-311++G(d,p) calculated relative electronic energies (ΔE_{el}), zero-point corrected electronic energies ($\Delta E_{(0)}$), and standard Gibbs energies ($\Delta G_{298.15}$) for the conformers of the *E*-enol-imine form of MHBAP, and their estimated room temperature gas-phase equilibrium conformational populations ($P_{298.15}$)

Conformer	ΔE_{el}	$\Delta E_{(0)}$	$\Delta G_{298.15}$	$P_{298.15}$[a]
I	0.41	0.51	0.63	14
II	34.9	33.3	30.5	
III	2.55	1.59	0.28	16
IV	2.54	1.72	0.62	14
V	0.00	0.00	0.00	18
VI	34.6	33.0	30.2	
VII	2.14	1.10	– 0.19	20
VIII	2.26	1.37	0.12	17
IX	45.9	43.6	41.3	
X	17.6	16.3	13.4	
XI	50.5	46.9	42.9	
XII	50.9	47.3	43.2	
XIII	45.6	43.3	40.9	
XIV	17.4	16.1	13.3	
XV	50.1	46.4	42.3	
XVI	50.6	50.0	42.9	

Energies in kJ mol^{-1} relative to conformer V. See Fig. 1, for structures of the conformers

[a]Altogether, the estimated population of conformers II, VI and IX–XVI is about 1%

(with and without inclusion of the zero-point correction) and standard Gibbs energies (at 298.15 K) of the conformers of the *E*-enol-imine MHBAP form, and their estimated populations in the room temperature (RT) gas-phase equilibrium. The conformationally relevant dihedral angles for the *E*-enol-imine conformers are given in Table 2, and those for the conformers of the other isomeric forms of MHBAP are provided in Table S2 (Supporting Material).

As presented in Table 1, the conformers of the *E*-enol-imine MHBAP isomer can be divided in two groups. The first group includes the more stable conformers, I, III, IV, V, VII and VIII, which share as common structural feature the presence of a stabilizing intramolecular OH···N hydrogen bond, established between the hydroxyl group of methoxy-substituted phenol moiety and the nitrogen atom of azomethine bridge. The second group is formed by all the other conformers, where this hydrogen bond is not present. This latter group may be divided into three subgroups, one formed by conformers X and XIV, which have energies (zero-point corrected) about 16 kJ mol^{-1} higher than the most stable conformer, the second by conformers II and VI, with relative energies to the most stable conformer around 33 kJ mol^{-1}, and the last one by conformers IX, XI, XII, XIII, XV and XVI, which have relative energies in the range 43–50 kJ mol^{-1} and where a strong OH···H repulsion is present. Conformers X and XIV are stabilized by the presence of a weak OH···O(CH_3) hydrogen bond (calculated H···O distance ~ 2.0 Å) and also of a favorable bond-dipole/bond-dipole interaction involving the C–H bond of the azomethine bridge and the C–O(H) bond, which are nearly antiparallelly polarized. The OH···O(CH_3) hydrogen bond is also present in conformers II and VI, but in these two cases the additional stabilizing bond-dipole/bond-dipole interaction that exists in conformers X and XIV is replaced by a repulsive interaction

Table 2 B3LYP/6-311++G(d,p) optimized conformationally relevant dihedral angles (in degrees) of the *E*-enol-imine conformers of MHBAP

Conformer	C–C=N–C	C=C–N=C δ	N=C–C=C ε	C=C–O–H α	C=C–O–H β	C=C–O–CH_3 γ
I	– 177.0	– 148.0	– 179.5	– 0.4	– 0.1	0.1
II	– 177.0	– 144.8	– 177.6	– 0.6	179.5	– 0.6
III	– 177.2	– 148.0	– 178.2	– 0.6	– 0.1	– 120.4
IV	– 177.1	– 148.2	179.4	– 0.5	– 0.6	121.0
V	– 177.2	– 149.0	– 179.4	178.6	– 0.1	– 0.1
VI	– 177.1	– 145.9	– 177.7	178.3	179.4	– 0.7
VII	– 177.3	– 149.1	– 178.2	178.5	0.0	– 120.2
VIII	– 177.2	– 149.2	179.4	178.5	– 0.5	120.8
IX	– 175.4	– 145.1	10.4	– 0.7	8.8	0.1
X	– 177.2	– 148.3	0.7	– 1.0	179.8	0.2
XI	– 175.1	– 145.2	11.9	– 0.5	11.5	115.7
XII	– 175.9	– 145.6	8.8	– 0.4	4.8	– 111.7
XIII	– 175.6	– 146.0	10.1	178.1	8.4	0.2
XIV	– 177.2	– 149.2	1.0	178.5	179.9	0.4
XV	– 175.3	– 146.3	11.4	178.1	10.6	115.5
XVI	– 176.1	– 146.7	8.4	178.1	4.0	– 111.9

For definition of dihedral angles and structures of the conformers, see Fig. 1

between the lone-electron pairs of the N and hydroxyl O atoms (see Fig. 1).

According to the computations, only the six low-energy conformers are significantly populated in the room temperature (298.15 K) gas-phase equilibrium, with all the other conformers having vanishing populations and being unimportant in experimental terms. In all the six low-energy conformers, the establishment of the intramolecular H-bond leads to the formation of a nearly planar pseudoaromatic six-membered ring, which also favors the π-electron delocalization between the methoxy-substituted phenolic ring and the azomethine bridge. This structural feature can be easily demonstrated by comparing the calculated values of the C–C bond of the bridge in these conformers (1.451 Å) with those predicted for all the other conformers (1.464–1.466 Å), as well as with the typical values for a single and a double carbon–carbon bond (1.54 and 1.34 Å, respectively; 1.39 Å in benzene). These comparisons allow also to conclude that the C–C bond of the azomethine bridge in the MHBAP intramolecularly H-bonded conformers has a substantial degree of double bond.

The strength of the OH···N intramolecular hydrogen bond, as measured by its associated structural parameters (see Table 3), is predicted to be nearly identical in all the hydrogen-bonded conformers. In all these forms, the O–H bond length is considerably shorter than that of free phenolic OH group (0.962 Å), staying in the narrow range of 0.993–0.995 Å, while the H···N and O···N hydrogen bond distances are also within the constricted ranges of 1.720–1.734 Å and 2.619–2.628 Å, respectively.

The calculated zero-point corrected relative electronic energies and Gibbs energies (at RT) of the six low-energy conformers of MHBAP differ by less than 2 and 1 kJ mol^{-1}, respectively (see Table 1), and their expected populations in the RT gas-phase equilibrium stay between 14 and 20%. Among these conformers, the three conformers having the free phenolic OH group pointing to the opposite direction (*trans*) of the *p*-substituent of that ring (V, VII and VIII) have slightly low Gibbs energies at RT than the remaining three forms, where the orientation is *cis* (I, III, IV). Conformer V, where the methoxy group is aligned with the plane of the ring, has the lowest calculated electronic energy (both with or without zero-point correction) among all conformers, and conformer I, with the same orientation of the methoxy group (but different orientation of the free OH group), has the lowest calculated electronic energy (both with or without zero-point correction) among all *cis* conformers. For each pair of conformers differing only in the orientation of the free OH group (I and V; III and VII; IV and VIII), the *trans*-OH form has always a lower electronic energy (either uncorrected and zero-point corrected). It is worth noticing that the placement of the methoxy group out of the ring plane leads to an increase of the entropy of the molecule (the calculated entropies at RT for conformers I and V are ~ 530 J mol^{-1} K^{-1}, while those of conformers III, IV, VII and VIII are within the 536–537 J mol^{-1} K^{-1} range). This results in a decrease of the Gibbs energies of the conformers bearing the methoxy substituent out of the ring plane compared to those where the methoxy group is aligned with the ring plane, and makes conformers VII and III to have the smallest Gibbs energy among all conformers and within the *cis* conformers, respectively.

Contrarily to the methoxy-substituted phenol ring that is nearly coplanar with the azomethine bridge, the second phenolic ring is deviated from the main plane of the molecule in all conformers of the *E*-enol-imine form of MHBAP (the same is also observed for the remaining forms of the compound, see Table S2 provided in the Supporting Material). This is caused by the repulsive interaction between the azomethine hydrogen atom and the closest located hydrogen atom of the phenolic moiety (see Fig. 1). In the six low-energy conformers, the phenol ring deviates from the planarity ~ 31°, which can be expected to reduce the π-electron delocalization between the phenol and azomethine

Table 3 B3LYP/6-311++G(d,p) selected calculated geometrical parameters of the low-energy intramolecularly H-bonded *E*-enol-imine conformers

	I	III	IV	V	VII	VIII
$O–H_{(H\text{-}bonded)}$	0.993	0.995	0.995	0.994	0.995	0.995
$O–H_{(free)}$	0.962	0.962	0.962	0.962	0.962	0.962
OH···N	1.734	1.721	1.722	1.732	1.720	1.721
O···N	2.628	2.620	2.620	2.627	2.619	2.620
C=N	1.288	1.288	1.288	1.288	1.288	1.288
C–C (bridge)	1.451	1.451	1.451	1.451	1.451	1.451
$C_{(phenol)}–N$	1.408	1.408	1.408	1.408	1.408	1.408
$C–OH_{(H\text{-}bonded)}$	1.337	1.342	1.342	1.337	1.342	1.343
$C–OH_{(free)}$	1.368	1.368	1.368	1.368	1.368	1.368
$C–OCH_3$	1.359	1.370	1.369	1.359	1.370	1.370
OH···N	147.7	148.0	148.0	147.8	148.1	148.1

Bond lengths and distances in Å; angles in degrees

fragments. Nevertheless, the calculated $C_{(phenol)}$–N bond length in these MHBAP conformers is 1.408 Å, which is only slightly longer than that found in aniline (1.407 Å [32]).

To estimate the energy barriers for conformational interconversions between the low-energy conformers of MHBAP, relaxed potential energy scans were performed along the relevant coordinates, at the B3LYP/6-311++G(d,p) level of theory. The six low-energy conformers of the compound (I, III, IV, V, VII and VIII) can be interconverted by several ways: (1) by rotation of non-hydrogen-bonded phenolic OH group (I ↔ V; III ↔ VII; IV ↔ VIII), (2) by rotation of the methoxy group (I ↔ III ↔ IV; V ↔ VII ↔ VIII), and (3) by rotation of around C–N bond connecting the phenol group bearing the free OH group to the azomethine bridge, which interconverts the same conformers as the rotation of the free phenolic OH group itself (I ↔ V; III ↔ VII; IV ↔ VIII). The potential energy profiles for the different interconversion pathways are depicted in Figs. 2, 3 and 4.

Figure 2 shows the potential energy profiles for the interconversions within the two groups of conformers differing by the orientation of the methoxy group (the *cis*-OH forms I, III and IV, in one side, and the *trans*-OH forms V, VII and VIII, in the other). When taken in the direction from the higher energy conformer to the lower energy form, all the barriers are of ca. 7 kJ mol^{-1} (as measured from the bottom of the potential wells). These barriers can be considered high enough for blocking any conformational conversion during deposition of the cryogenic matrices [33, 34], so that conformers with all the 3 possible orientations of the methoxy group can be expected to be present in the as-deposited cryogenic matrices.

The interconversion by direct rotamerization of the free OH group in the three related pairs of conformers (I ↔ V; III ↔ VII; IV ↔ VIII) takes place through energy barriers of ca. 14 kJ mol^{-1} (Fig. 3). These barriers are also high enough to prevent occurrence of the over-the-barrier transformations at the cryogenic temperature used in the matrix isolation experiments (10 K) [33, 34]. However, H-atom quantum mechanical tunneling through a barrier of such height may take place with a high probability, as it has been observed to happen in other phenolic and similar compounds carrying hydroxyl groups [4, 35, 36], and this possibility must be considered when interpreting the results of the matrix isolation experiments described in the next section.

On the other hand, the I ↔ V, III ↔ VII and IV ↔ VIII conformational conversions through rotation of around C–N bond connecting the phenol group bearing the free OH group to the azomethine bridge imply to overcome barriers of ca. 10 kJ mol^{-1} (Fig. 4), which are also enough high to allow the different conformers to be trapped in the cryogenic matrices during deposition. It is interesting to note that the barriers separating either conformer V from its symmetrically-related structure as well as those between III and IV' (or III' and IV) and VII and VIII' (or VII' and VIII) forms are rather low (< 3 kJ mol^{-1}), though they are clearly above the zero-point level at the geometry of the minima (~ 0.5 kJ mol^{-1}), so that all equivalent-by-symmetry structures correspond effectively to true degenerated conformational forms.

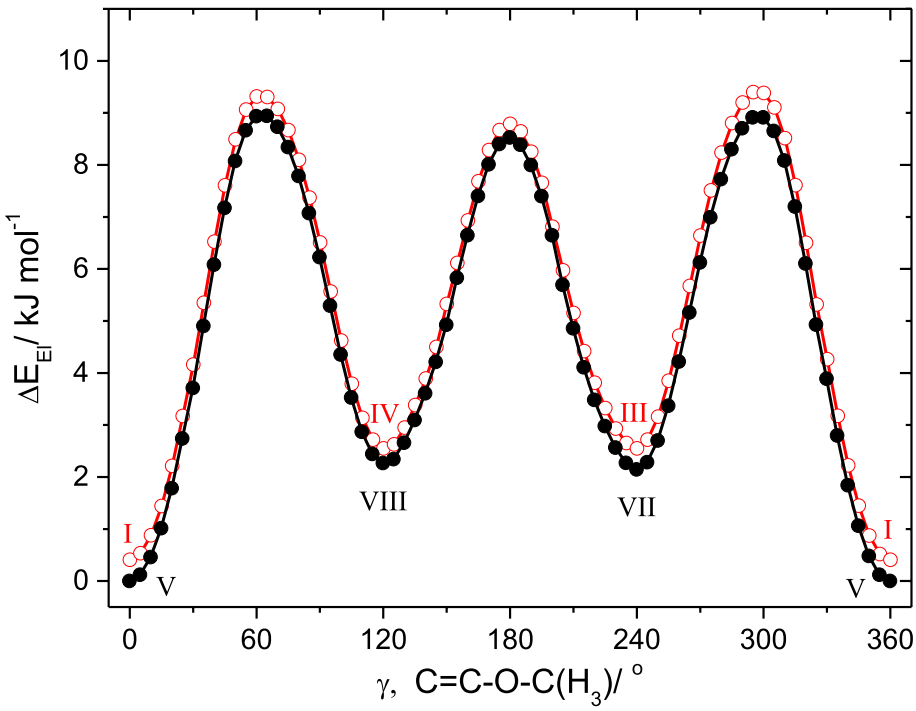

Fig. 2 Potential energy profiles for interconversions I ↔ III ↔ IV and V ↔ VII ↔ VIII resulting from internal rotation around the C-O(CH_3) bond

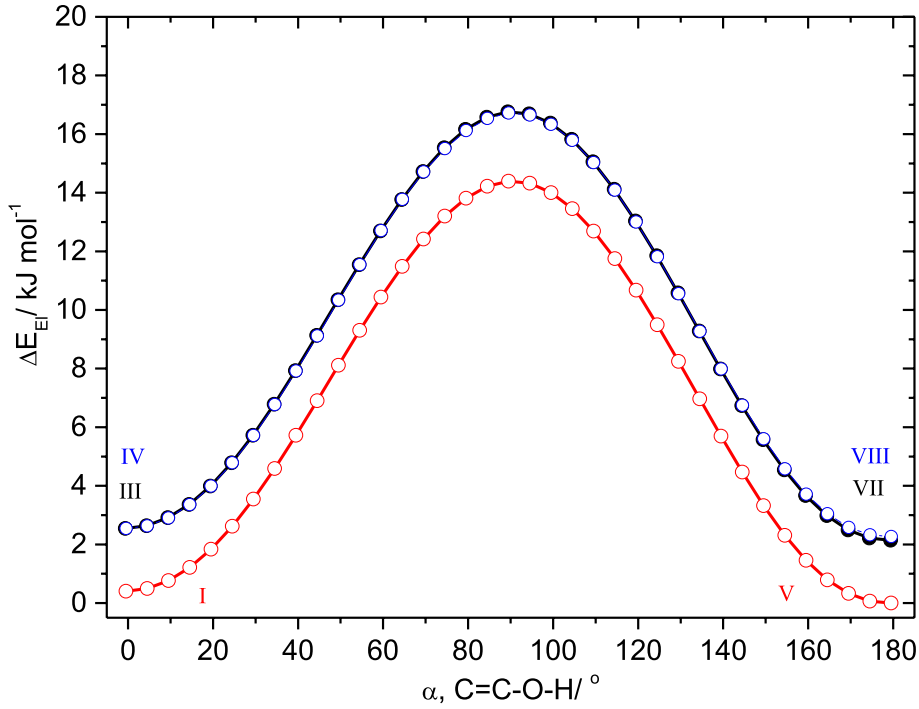

Fig. 3 Potential energy profiles for interconversions I ↔ V, III ↔ VII and IV ↔ VIII resulting from internal rotation around the C–$O(H)_{free}$ bond

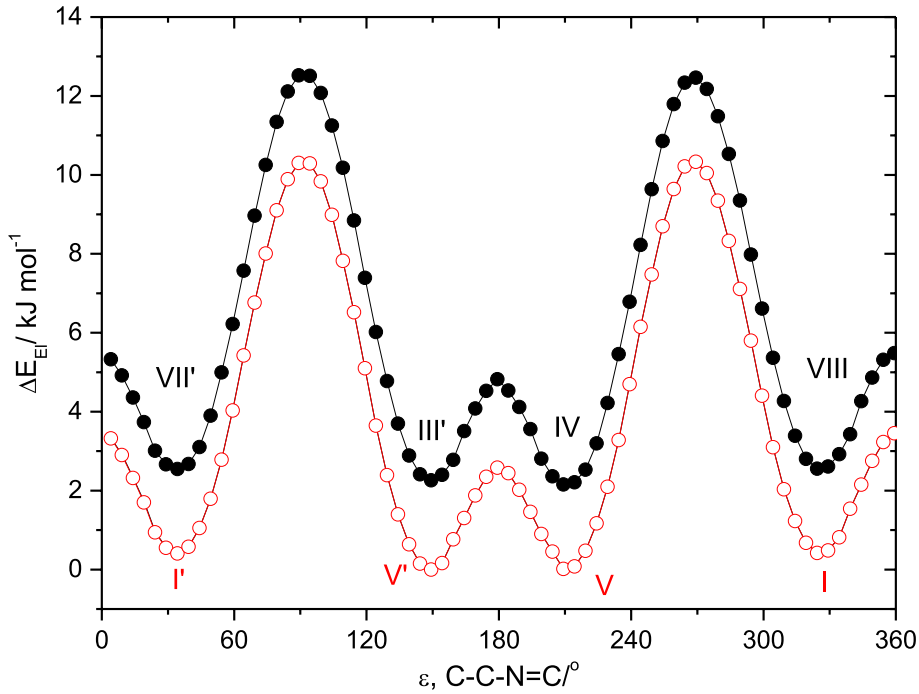

Fig. 4 Potential energy profiles for interconversions I′ ↔ V′ ↔ V ↔ I and VII′ ↔ III′ ↔ IV ↔ VIII resulting from internal rotation around the C–N bridging bond. The symbol' refers to the symmetry-related structures of the conformers depicted in Fig. 1

3.2 Matrix isolation infrared experiments

Molecules of MHBAP were isolated in a cryogenic (10 K) argon matrix from the RT gas-phase. The infrared spectrum of the as-deposited matrix is shown in Fig. 5. As discussed in the previous section, according to the performed DFT calculations the six low-energy intramolecularly H-bonded conformers of the *E*-enol-imine form of MHBAP are present in the gas-phase prior to deposition with populations ranging from 14 to 20% (see Table 1). Nevertheless, as mentioned above, the low energy barrier for rotamerization of the free OH group can be expected to allow for quantum mechanical tunneling conversion between the conformers differing only in the orientation of

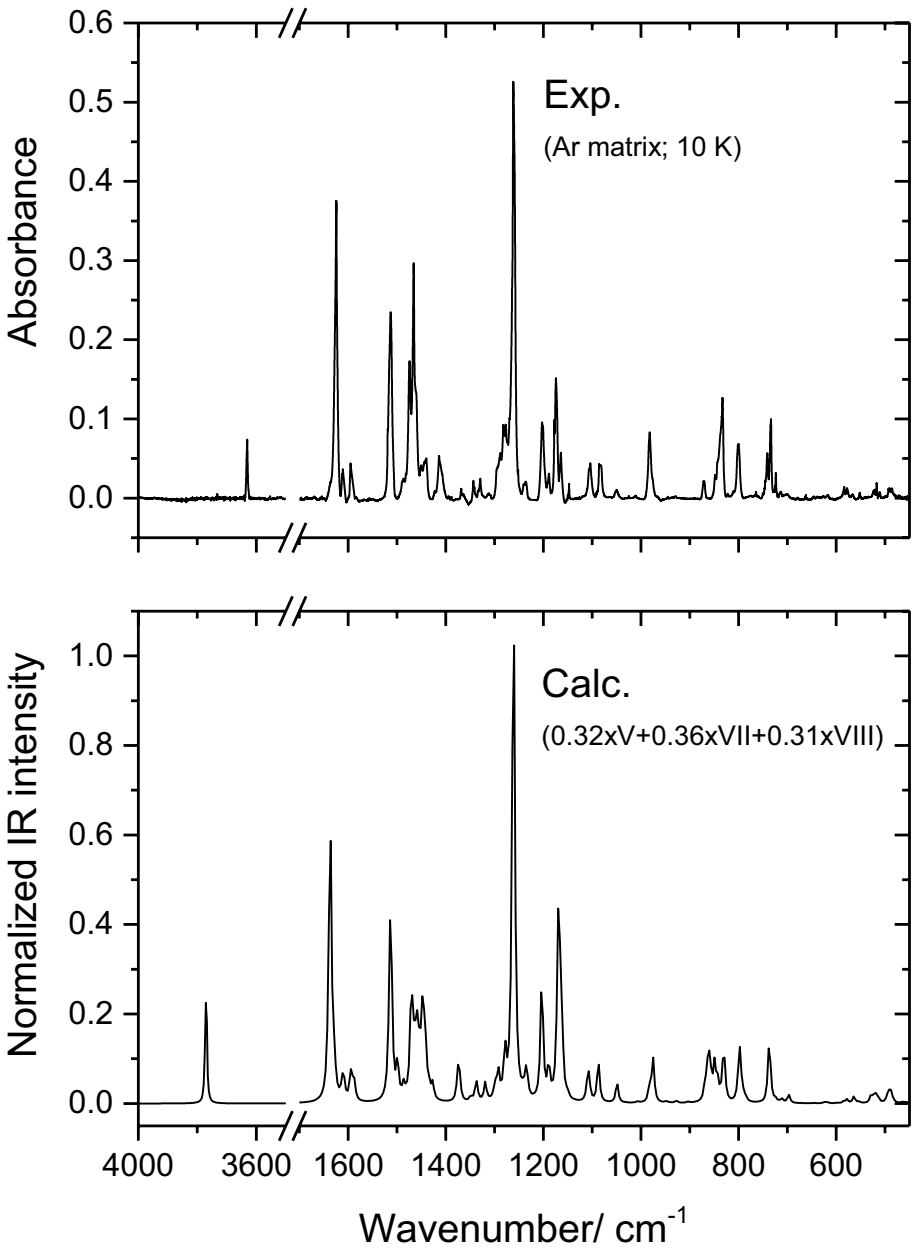

Fig. 5 *Top panel:* As-deposited infrared spectrum of MHBAP isolated in an argon matrix (10 K); *Lower panel*: Simulated infrared spectrum built using the calculated infrared spectra of conformers V, VII and VIII weighted by the estimated populations in the matrix, taking into account the free OH tunneling during deposition (see text for details). Calculated wavenumbers were scaled as described in Sect. 2

this group, so that from each pair (I and V, III and VII and IV and VIII), only the lower energy *trans*-OH form should be trapped in the cryogenic matrix. Figure 5 presents also the simulated infrared spectrum constructed by adding the DFT(B3LYP)/6-311++G(d,p) calculated infrared spectra of conformers V, VII and VIII weighted by the sum of their expected populations in the matrix after conversion of the corresponding *cis*-OH forms into these conformers (32%, 36% and 31%, for V, VII and VIII, respectively). As it can be seen, the agreement between the experimental and the simulated spectra is excellent, a result that agrees with the conclusions extracted from the data obtained from the DFT calculations that only the three *trans*-OH low-energy intramolecularly H-bonded *E*-enol-imine conformers of MHBAD should be present in the as-deposited matrix of the compound. In the Supporting Material (Figure S9) the experimental spectrum is compared with those of the most stable conformer of the high-energy *Z*-enol-imine and both keto-amino forms of the compound, which clearly do not fit well the experimental data.

A tentative spectra assignment was undertaken, and the results are summarized in Table S3, in the Supporting Material. The assignments were supported by the comparison of the experimental spectrum with the calculated ones, and also taking into account the results of the UV-irradiation experiments described below, which allowed for separation

of bands due to conformer V from those originated in conformers VII and VIII.

The as-deposited matrix of MHBAP was submitted to UV irradiation ($\lambda = 230$ nm; ~ 15 mW at the sample). The difference spectrum obtained by subtracting the infrared spectrum of the as-deposited matrix from that recorded after 45 min of irradiation in shown in Fig. 6. Irradiations performed at 275 and 335 nm were also undertaken and the results obtained were essentially identical to those obtained upon irradiation at 230 nm.

The difference spectrum clearly shows a redistribution of intensities of the bands originally present in the as-deposited spectrum. Detailed comparison of the experimental results with the calculated spectra of the conformers initially present in the matrix (V, VII and VIII), allowed us to conclude that the UV irradiation promotes rotamerization of the methoxy group, converting the lowest energy conformer V, where the methoxy group is aligned with the plane of the ring, into conformers VII and VIII, in which the OCH_3 group is out-of-the-plane of the ring. The simulated spectrum corresponding to this transformation is presented in the lower panel of Fig. 6, and it shows an excellent agreement with the experimental difference spectrum.

The observed phototransformation is similar to that previously observed for 6-methoxyindole isolated in argon and xenon matrices [37], where rotamerization of the methoxy substituent was successfully induced upon UV irradiation in the 300–305 nm range. In 6-methoxyindole, the

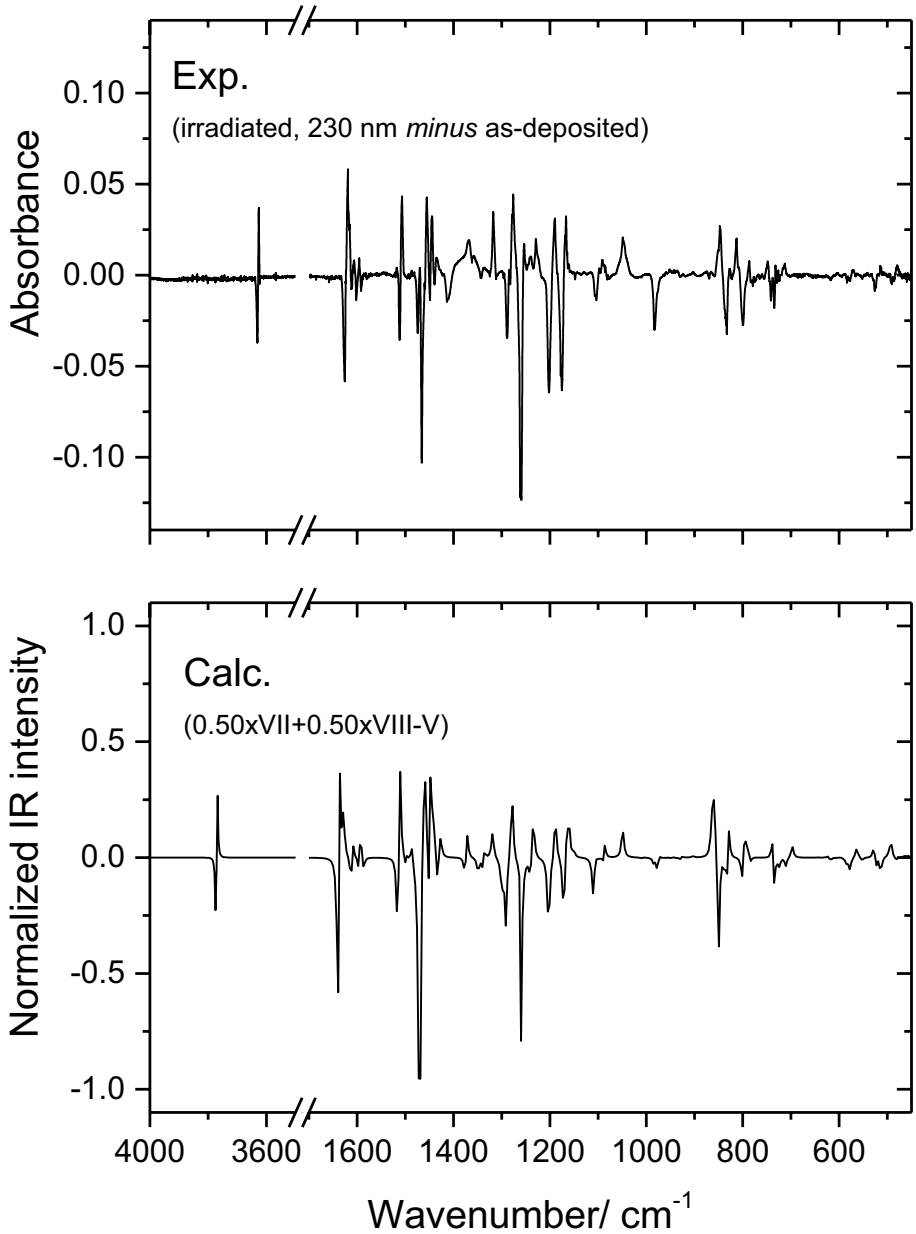

Fig. 6 Top panel: infrared difference spectrum (spectrum of matrix isolated MHBAP recorded after 45 min of UV-irradiation at 230 nm minus as-deposited spectrum); Lower panel: simulated infrared difference spectrum ($0.5 \times \text{VII} + 0.5 \times \text{VIII} - \text{V}$)

methoxy rotamerization barrier has been predicted to be 9–10 kJ mol^{-1} [38], which is similar to that found in the present study for the V → VII and V → VIII conversions (~7 kJ mol^{-1}; see Fig. 2).

The possibility of occurrence of other photoinduced processes was evaluated. Photoproduction of any of the higher energy isomeric forms of MHBAP (in particular the keto-amine forms that would result from excited state proton transfer) as well as any other species resulting from a rearrangement or fragmentation was easily excluded, since no new bands appeared in the spectrum after irradiation. The same applies to the production of other conformers of the *E*-enol-imine form of the compound. The most striking result is the non-observation of any conformer that could result from internal rotations about the C–N bond connecting the phenol group bearing the free OH group to the azomethine bridge, or from direct rotamerization of the free OH group. In both cases, as discussed before, *cis*-OH conformers would be produced, in particular the low-energy conformers I, III and IV, which would result from the *trans*-OH conformers V, VII and VIII, respectively. These processes looked very much possible to take place upon UV-irradiation, considering the low associated barriers of only 10 and 14 kJ mol^{-1} (see Figs. 3, 4). In fact, the occurrence of such processes cannot be excluded. However, if the *cis*-OH conformers (I, III, IV) are formed, they promptly convert to the corresponding *trans*-OH forms (V, VII, VIII) by fast quantum mechanical tunneling, and cannot be observed experimentally. As mentioned before, occurrence of this fast OH tunneling is a general rule in case of phenol compounds and has been systematically observed before [4, 35, 36].

4 Conclusion

The UV-induced (λ = 230 nm) –OCH_3 rotamerization in a matrix-isolated new methoxy-substituted *ortho*-hydroxyaryl Schiff base compound, 4-(3-methoxy-2-hydroxybenzylideneamino) phenol was observed, leading to the conversion of the lowest energy *trans*-OH *E*-enol-imine conformer V of the compound, where the methoxy group is aligned with the plane of the ring, into the two other *trans*-OH conformers initially present in the argon matrix (VII and VIII), in which the OCH_3 group is out-of-the-plane of the ring.

The compound was synthesized from 4-aminophenol and 2-hydroxy-3-methoxybenzaldehyde in methanol solution and characterized by ^{1}H- and ^{13}C-NMR and infrared spectroscopies and elemental analysis. After isolation in a cryogenic (10 K) argon matrix from the RT gas-phase equilibrium, three different conformers were detected in the as-deposited matrix by infrared spectroscopy. These conformers (V, VII and VIII) of the lowest energy *E*-enol-imine isomer of the compound have the free hydroxyl group in the *trans* orientation relatively to the *para*-substituent of the ring and possess an OH···N intramolecular hydrogen bond involving the OH group of the methoxy-substituted phenol ring and the azomethine bridge, and differ in the orientation of the OCH_3 substituent. As in the case of other phenolic compounds previously studied, spontaneous quantum mechanical tunneling conversion of the *cis*-OH conformers present in the gas-phase before deposition (I, III, IV) into the three observed structurally related conformers (V, VII and VIII, respectively) was found to take place during matrix deposition, which precludes observation of these forms in the matrix conditions. It is also possible that the UV-irradiation also leads to formation of the *cis*-OH forms, but once formed, they promptly relax to the lower-energy *trans*-OH forms (I → V, III → VII, IV → VIII), preventing their observation. The structures and relative energies of the whole set of different conformers of the different isomers of the molecule (*E*- and *Z*-enol-imine and *E*- and *Z*-keto-amine forms), and relevant barriers for their conformational interconversion were also obtained through quantum chemical calculations performed at the DFT(B3LYP)/6-311++G(d,p) level of theory, which were also applied to predict the infrared spectra of the different conformers that were used to support the interpretation of the experimental data.

Supplementary Information The online version contains supplementary material available at https://doi.org/10.1007/s43630-021-00166-z.

Acknowledgements This work was supported by Project PTDC/QUI-QFI/1880/2020, funded by National Funds via the Portuguese Foundation for Science and Technology (FCT). The Coimbra Chemistry Centre is supported by FCT through projects UIDB/QUI/0313/2020 and UIDP/QUI/0313/2020, co-funded by COMPETE. This work was also supported by Project BEBAP-2013.05, funded by Bitlis Eren University Research Foundation.

Author contributions All authors contributed to the study conception and design, material preparation, data collection and analysis. The first draft of the manuscript was written by İsa Sıdır and all authors commented on previous versions of the manuscript. All authors read and approved the final manuscript.

Declarations

Conflict of interest The authors have no financial nor competing interests to disclose. All authors certify that they have no affiliations with or involvement in any organization or entity with any financial interest or non-financial interest in the subject matter or materials discussed in this manuscript. The authors have no financial or proprietary interests in any material discussed in this article.

References

1. Sıdır, Y. G., Pirbudak, G., Berber, H., & Sıdır, İ. (2017). Study on the electronic and photophysical properties of the substitute-((2-phenoxybenzylidene)amino)phenol derivatives: Synthesis,

solvatochromism, electric dipole moments and DFT calculations. *Journal of Molecular Liquids, 242*, 1096–1110.
2. Sıdır, Y. G., Berber, H., & Sıdır, İ. (2019). The dipole moments and solvatochromism of ((4-(benzyloxy)benzylidene)amino)phenol compounds as solvatochromic materials. *Journal of Solution Chemistry, 48*, 775–806.
3. Sıdır, Y. G., Aslan, C., Berber, H., & Sıdır, İ. (2019). The electronic structure, solvatochromism, and electric dipole moments of new Schiff base derivatives using absorbance and fluorescence spectra. *Structural Chemistry, 30*, 835–851.
4. Sıdır, İ, Sıdır, Y. G., Góbi, S., Berber, H., & Fausto, R. (2021). Structural relevance of intramolecular H-bonding in *ortho*-hydroxyaryl Schiff bases: the case of 3-(5-bromo-2-hydroxybenzylideneamino) phenol. *Molecules, 26*, 2814.
5. Avadanei, M., Cozan, V., Kuş, N., & Fausto, R. (2015). Structure and photochemistry of *N*-salicylidene-*p*-carboxyaniline ısolated in solid argon. *Journal of Physical Chemistry A, 119*, 9121–9132.
6. Melloni, A., Paccani, R. R., Donati, D., Zanirato, V., Sinicropi, A., Parisi, M. L., Martin, E., Ryazantsev, M., Ding, W. J., Frutos, L. M., Basosi, R., Fusi, E., Latterini, L., Ferré, N., & Olivucci, M. (2010). Modeling, preparation, and characterization of a dipole moment switch driven by *Z*/*E* photoisomerization. *Journal of the American Chemical Society, 132*, 9310–9319.
7. Staykov, A., Watanabe, M., Ishihara, T., & Yoshizawa, K. (2014). Photoswitching of conductance through salicylidene methylamine. *Journal of Physical Chemistry C, 118*, 27539–27548.
8. Dalapati, S., Jana, S., & Guchhait, N. (2014). Anion recognition by simple chromogenic and chromo-fluorogenic salicylidene Schiff base or reduced-Schiff base receptors. *Spectrochimica Acta Part A: Molecular Spectroscopy, 129*, 499–508.
9. Zhang, X., Yin, J., & Yoon, J. (2014). Recent advances in development of chiral fluorescent and colorimetric sensors. *Chemical Reviews, 114*, 4918–4959.
10. Wu, P., Bhamidipati, M., Coles, M., & Rao, D. V. G. L. N. (2004). Biological nano-ceramic materials for holographic data storage. *Chemical Physics Letters, 400*, 506–510.
11. Yuan, W., Sun, L., Tang, H., Wen, Y., Jiang, G., Huang, W., Jiang, L., Song, Y., Tian, H., & Zhu, D. A. (2005). Novel thermally stable spironaphthoxazine and its application in rewritable high density optical data storage. *Advanced Materials, 17*, 156–160.
12. Yanez, C. O., Andrade, C. D., Yao, S., Luchita, G., Bondar, M. V., & Belfield, K. D. (2009). Photosensitive polymeric materials for two-photon 3D WORM optical data storage systems. *ACS Applied Materials and Interfaces, 1*, 2219–2229.
13. Hadjoudis, E., & Mavridis, I. M. (2004). Photochromism and thermochromism of Schiff bases in the solid state: Structural aspects. *Chemical Society Reviews, 33*, 579–588.
14. Amimoto, K., & Kawato, T. (2005). Photochromism of organic compounds in the crystal state. *Journal of Photochemistry and Photobiology, C: Photochemistry Reviews, 6*, 207–226.
15. Jia, Y., & Li, J. (2015). Molecular assembly of Schiff base interactions: Construction and application. *Chemical Reviews, 115*, 1597–1621.
16. Wang, Z., Möhwald, H., & Gao, C. (2011). Preparation and redox-controlled reversible response of ferrocene-modified poly(allylamine hydrochloride) microcapsules. *Langmuir, 27*, 1286–1291.
17. Wang, B., Xu, C., Xie, J., Yang, Z., & Sun, S. (2008). pH controlled release of chromone from chromone–Fe_3O_4 nanoparticles. *Journal of the American Chemical Society, 130*, 14436–14437.
18. Duan, L., Qi, W., Yan, X., He, Q., Cui, Y., Wang, K., Li, D., & Li, J. (2009). Proton gradients produced by glucose oxidase microcapsules containing motor F0F1-ATPase for continuous ATP biosynthesis. *The Journal of Physical Chemistry B, 113*, 395–399.
19. Avadanei, M., Cozan, V., Shova, S., & Paixão, J. A. (2014). Solid state photochromism and thermochromism of two related *N*-salicylidene anilines. *Chemical Physics, 444*, 43–51.
20. Minkin, V. I., Tsukanov, A. V., Dubonosov, A. D., & Bren, V. A. (2011). Tautomeric Schiff bases: Iono- solvato-, thermo- and photochromism. *Journal of Molecular Structure, 998*, 179–191.
21. Filarowski, A., Głowiaka, T., & Koll, A. (1999). Strengthening of the intramolecular O···H···N hydrogen bonds in Schiff bases as a result of steric repulsion. *Journal of Molecular Structure, 484*, 75–89.
22. Filarowski, A., Koll, A., & Głowiak, T. (2003). Structure and hydrogen bonding in ortho-hydroxy ketimines. *Journal of Molecular Structure, 644*, 187–195.
23. Filarowski, A., Koll, A., Karpfen, A., & Wolschann, P. (2004). Intramolecular hydrogen bond in molecular and proton-transfer forms of Schiff bases. *Chemical Physics, 297*, 323–332.
24. Becke, A. D. (1988). Density-functional exchange-energy approximation with correct asymptotic behavior. *Physical Review A, 38*, 3098–3100.
25. Lee, C., Yang, W., & Parr, R. G. (1988). Development of the Colle-Salvetti correlation-energy formula into a functional of the electron density. *Physical Review B, 37*, 785–789.
26. Vosko, S. H., Wilk, L., & Nusair, M. (1980). Accurate spin-dependent electron liquid correlation energies for local spin density calculations: a critical analysis. *Canadian Journal of Physics, 58*, 1200–1211.
27. McLean, A. D., & Chandler, G. S. (1980). Contracted Gaussian basis sets for molecular calculations. I. Second row atoms, Z = 11–18. *Journal of Chemical Physics, 72*, 5639–5648.
28. Raghavachari, K., Binkley, J. S., Seeger, R., & Pople, J. A. (1980). Self-consistent molecular orbital methods. XX. A basis set for correlated wave functions. *Journal of Chemical Physics, 72*, 650–654.
29. Frisch, M. J., Pople, J. A., & Binkley, J. S. (1984). Self-consistent molecular orbital methods 25. Supplementary functions for Gaussian basis sets. *Journal of Chemical Physics, 80*, 3265–3269.
30. Frisch, M. J., Trucks, G. W., Schlegel, H. B., Scuseria, G. E., Robb, M. A., Cheeseman, J. R., Scalmani, G., Barone, V., Mennucci, B., Petersson, G. A., et al. (2009). *Gaussian 09, Revision D.01*. Wallingford: Gaussian, Inc.
31. ChemCraft (version 1.8) (2021)—Graphical software for visualization of quantum chemistry computations. https://www.chemcraftprog.com.
32. Zhang, H., Jiang, X., Wu, W., & Mo, Y. (2016). Electron conjugation versus π–π repulsion in substituted benzenes: Why the carbon-nitrogen bond in nitrobenzene is longer than in aniline. *Physical Chemistry Chemical Physics: PCCP, 18*, 11821–11828.
33. Reva, I., Simão, A., & Fausto, R. (2005). Conformational properties of trimethyl phosphate monomer. *Chemical Physics Letters, 406*, 126–136.
34. Reva, I. D., Lopes Jesus, A. J., Rosado, M. T. S., Fausto, R., Eusébio, M. E., & Redinha, J. S. (2006). Stepwise conformational cooling towards a single isomeric state in the four internal rotors system 1,2-butanediol. *Physical Chemistry Chemical Physics: PCCP, 8*, 5339–5349.
35. Nanbu, S., Sekine, M., & Nakata, M. (2011). Hydrogen-atom tunneling in isomerization around the C–O bond of 2-chloro-6-fluorophenol in low-temperature argon matrixes. *Journal of Physical Chemistry A, 115*, 9911–9918.
36. Kuş, N., Sagdinc, S., & Fausto, R. (2015). Infrared spectrum and UV-induced photochemistry of matrix-isolated 5-hydroxyquinoline. *Journal of Physical Chemistry A, 119*, 6296–6308.
37. Lopes Jesus, A. J., Reva, I., & Fausto, R. (2017). UV-induced transformations in matrix-isolated 6-methoxyindole. *Journal of Photochemistry and Photobiology A: Chemistry, 336*, 123–130.
38. Lopes Jesus, A. J., Reva, I., & Fausto, R. (2016). Conformational changes in matrix-ısolated 6-methoxyindole: effects of the thermal and ınfrared light excitations. *Journal of Chemical Physics, 144*(1–9), 124306.

Authors and Affiliations

İsa Sıdır[1,2] · Yadigar Gülseven Sıdır[1,2] · Sándor Góbi[2,3] · Halil Berber[4] · Gulce Ogruc Ildiz[5] · Rui Fausto[2]

✉ İsa Sıdır
isidir@beu.edu.tr

✉ Rui Fausto
rfausto@ci.uc.pt

[1] Department of Physics, Faculty of Science and Arts, Bitlis Eren University, 13000 Bitlis, Turkey

[2] CQC-IMS, Department of Chemistry, University of Coimbra, 3004-535 Coimbra, Portugal

[3] MTA-ELTE Lendület Laboratory Astrochemistry Research Group, Institute of Chemistry, ELTE Eötvös Loránd University, H-1518 Budapest, Hungary

[4] Department of Chemistry, Faculty of Science, Eskişehir Technical University, 26470 Eskişehir, Turkey

[5] Department of Physics, Faculty of Sciences and Letters, Istanbul Kultur University, 34158 Bakırkoy, Istanbul, Turkey